Conformational Analysis of the Eight-Membered Ring of the Oxidized Cysteinyl-Cysteine Unit Implicated in Nicotinic Acetylcholine Receptor Ligand Recognition

Christopher J. Creighton, Charles H. Reynolds, Daniel H. S. Lee,‡ Gregory C. Leo,* and Allen B. Reitz*

Contribution from the Drug Discovery Division, R. W. Johnson Pharmaceutical Research Institute, Welsh and McKean Roads, P.O. Box 776, Spring House, Pennsylvania 19477-0776

Received June 27, 2001

Abstract: Nicotinic acetylcholine receptors (nAChRs) are membrane-bound, pentameric ligand-gated ion channels associated with a variety of human disorders such as Alzheimer's disease, Parkinson's disease, schizophrenia, and pain. Most known nAChRs contain an unusual eight-membered disulfide-containing cysteinyl-cysteine ring, *ox*-[Cys-Cys], as does the soluble acetylcholine binding protein (AChBP) found in the snail *Lymnaea stagnalis*. The cysteinyl-cysteine ring is located in a region implicated in ligand binding, and conformational changes involving this ring may be important for modulation of nAChR function. We have studied the preferred conformations of Ac-*ox*-[Cys-Cys]-NH_2 by NMR in water and computationally by Monte Carlo simulations using the OPLS-AA force field and GB/SA water model. *ox*-[Cys-Cys] adopts four distinct low-energy conformers at slightly above 0 °C in water. Two populations are dependent on the peptide ω_2 dihedral angle, with the trans amide favored over the cis amide by a ratio of ca. 60:40. Two *ox*-[Cys-Cys] conformers with a cis amide bond (C+ and C−) differ from each other primarily by variation of the χ_3 dihedral angle, which defines the orientation of the helicity about the S−S bond (± 90°). Two trans amide conformers have the same S−S helicity ($\chi_3 \approx -90°$), but are distinguished by a backbone rotation about ϕ_2 and ψ_1 (T− and T′−). The ratio of T−/T′−/C+/C− is 47:15:29:9. The orientation of the pendant moieties from the eight-membered ring is more compact for the major trans conformer (T−) than for the extended conformations adopted by T′−, C+, and C−. These conformational preferences are also observed in tetrapeptide and undecapeptide fragments of the human α_7 subtype of the nAChR that contains the *ox*-[Cys-Cys] unit. Conformer T− is nearly identical to the conformation seen in the X-ray structure of *ox*-[Cys^{187}-Cys^{188}] found in the unliganded AChBP, and is a Type VIII β-turn.

Nicotinic acetylcholine receptors (nAChRs) are important membrane-bound, pentameric ligand-gated ion channels that mediate intracellular communication.[1] Neuronal nAChRs such as the α_7 and $\alpha_4\beta_2$ subtypes have been implicated in a variety of debilitating human disorders including Alzheimer's disease, Parkinson's disease, and pain. The α_7 receptor subtype is unique in that the five protein subunits are comprised of the identical α_7 protein. For typical nAChRs, a binding epitope for nicotine, acetylcholine, and the curaremimetic neurotoxin α-bungarotoxin is located ca. 200 residues from the *N*-terminus in the extracellular portion of the receptor.[2] β-Amyloid$_{1-40(42)}$ peptides, involved in the etiology of Alzheimer's disease (AD),[3] bind selectively and with high affinity to the α_7 nAChR.[4] The α_7 nAChR mediates calcium homeostasis and ACh release. The interaction of amyloid peptides with the α_7 nAChR may exacerbate the cholinergic deficits that characterize AD, and promote a long-term decline in cognitive performance.[5] Understanding the preferred conformations of regions of the AChRs that recognize ligands such as ACh, nicotine, and β-amyloid may provide insight for the design of new therapeutic agents to treat AD and other disorders.

An unusual oxidized eight-membered-ring disulfide *ox*-[Cys-Cys] (**1**) is found in the *N*-terminal extracellular domain of most nAChR protein subtypes (Figure 1).[6] Conformational changes involving this ring have been proposed to play a role in modulating nAChR function. These changes occur upon the binding of ACh,[7] although the binding of α-bungarotoxin is

* To whom correspondence should be addressed: areitz@prius.jnj.com and gleo@prius.jnj.com.

‡ Present address: Biogen Inc., Cambridge, MA.

(1) Holladay, M. W.; Dart, M. J.; Lynch, J. K. *J. Med. Chem.* **1997**, *40*, 4169−4194.

(2) (a) Testai, F. D.; Venera, G. D.; Peña, C.; d. J. Bonino, M. J. B. *Neurochem. Int.* **2000**, *36*, 27−33. (b) McLane, K. E.; Wu, X.; Conti-Tronconi, B. M. *Biochemistry* **1994**, *33*, 2576−2585. (c) McLane, K. E.; Wu, X.; Diethelm, B.; Conti-Tronconi, B. M. *Biochemistry* **1991**, *30*, 4925−4934. (d) Lentz, T. L. *Biochem. Biophys. Res. Commun.* **2000**, *268*, 480−484. (e) Lentz, T. L.; Chaturvedi, V.; Conti-Fine, B. M. *Biochem. Pharmacol.* **1998**, *55*, 341−347. (f) Lentz, T. L. *Biochemistry* **1995**, *34*, 1316−1322. (g) Wilson, P. T.; Lentz, T. L.; Hawrot, E. *Proc. Natl. Acad. Sci., U.S.A.* **1985**, *82*, 8790−8794. (h) Antil-Delbeke, S.; Gaillard, C.; Tamiya, T.; Corringer, P.-J.; Changeux, J.-P.; Servent, D.; Ménez, A. *J. Biol. Chem.* **2000**, *275*, 29594−29601.

(3) Cotman, C. W.; Cribbs, D. H.; Anderson, A. J. In *Molecular Mechanisms of Dementia*; Wasco, W., Tanzi, R. E., Eds.; Humana Press: Totowa, NJ, 1997; pp 73−90.

(4) (a) Wang, H.-Y.; Lee, D. H. S.; D'Andrea, M. R.; Peterson, P. A.; Shank, R. P.; Reitz, A. B. *J. Biol. Chem.* **2000**, *275*, 5626−5632. (b) Wang, H.-Y.; Lee, D. H. S.; Davis, C. B.; Shank, R. P. *J. Neurochem.* **2000**, *75*, 1155−1161.

(5) (a) Liu, Q.-S.; Kawai, H.; Berg, D. K. *Proc. Natl. Acad. Sci., U.S.A.* **2001**, *98*, 4734−4739. (b) Petit, D. L.; Shao, Z.; Yakel, J. L. *J. Neurosci.* **2001**, *21*, RC120. (c) Dineley, K. T.; Westerman, M.; Bui, D.; Bell, K.; Ashe, K. H.; Sweatt, J. D. *J. Neurosci.* **2001**, *21*, 4125−4133.

(6) Le Novère, N.; Corringer, P.-J.; Changeux, J.-P. *Biophys. J.* **1999**, *76*, 2329−2345.

10.1021/ja016505m CCC: $20.00
Published on Web 11/22/2001

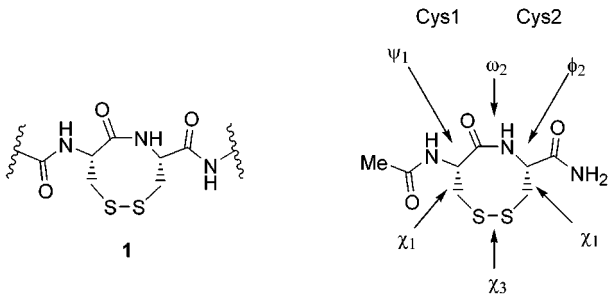

1 2

Ac-Glu-*ox*-[Cys-Cys]-Lys-NH_2

3

Ac-Ser-Glu-Arg-Phe-Tyr-Glu-*ox*-[Cys-Cys]-Lys-Glu-Pro-NH_2

4

Figure 1. Structures of *ox*-[Cys-Cys] (**1**), Ac-*ox*-[Cys-Cys]-NH_2 (**2**), human α_7 nAChR$^{211-214}$ (**3**), and human α7 nAChR$^{206-216}$ (**4**).

not affected by the state of oxidation of the Cys-Cys unit.[2c,8] The binding of the natural ligand ACh is sensitive to the state of oxidation of the two cysteines,[9] and mutation of either cysteine to a serine results in loss of ACh binding and a closed ion channel.[10] Disulfide **1** is also found in the catalytic domain of mercuric ion reductase,[11] and *ox*-[D-Cys-D-Cys] in the bicyclic peptide malformin.[12]

A soluble acetylcholine binding protein (AChBP) from glial cells has recently been characterized. The AChBP has a high level of sequence homology with the *N*-terminal, extracellular domain of typical nAChR α subunits.[13] The X-ray structure of AChBP reveals a cylindrical arrangement of five identical proteins.[14] The characteristic *ox*-[Cys^{187}Cys^{188}] subunit is located in a cleft between two adjacent subunits. The position and orientation of the *ox*-[Cys-Cys] structure in the AChBP are consistent with a possible role as a fulcrum for transitions between significantly different protein conformations with corresponding effects upon function.

Previous conformational analysis of the *ox*-[Cys-Cys] ring has been conducted in organic solvents,[15] in mixed aqueous/organic solvents,[7b] or in an aqueous environment but at low-field NMR strength.[15a] Interpretation of the data found in these earlier studies was often complicated by poor spectral resolution. It was postulated that the complex spectrum observed for *ox*-[Cys-Cys] in DMSO-d_6 was due to simultaneous isomerization about the amide bond and interconversion of the helicity expected for the disulfide bond.[15b] A pentapeptide containing *ox*-[Cys-Cys] incorporated in the sequence TCCPD, a fragment from the *Torpedo* nAChR, has been studied to the greatest extent.[7b] This work did not provide detailed structural insight involving the trans amide conformers, partly because of the added structural complexity imparted by the *C*-terminal proline.

We present here a complete conformational analysis of the model peptide Ac-*ox*-[Cys-Cys]-NH_2 (**2**) in water and limited studies of tetrapeptide (**3**) and undecapeptide (**4**) which are fragments of the α_7 nAChR. Of the eight dihedral angles that define the *ox*-[Cys-Cys] system, the amide angle (ω_2) is reasonably expected to adopt two orientations (0° or 180°) and the disufide (χ_3) two as well (ca. $\pm$ 90°). We utilized homonuclear and heteronuclear scalar coupling constants and the Karplus equation[16] to determine ϕ_2 and the two χ_1 angles of each of the conformers of *ox*-[Cys-Cys]. We also used Monte Carlo calculations to identify low-energy conformations for Cys-Cys. These computed structures were matched to the NMR data in order to assign the four conformers observed experimentally.

Results and Discussion

NMR Studies. Analysis of the ^{1}H NMR spectra of Ac-*ox*-[Cys-Cys]-NH_2 (**2**) dissolved in water revealed many more peaks than expected for a simple dipeptide. The lowest possible temperature without freezing the sample was used to sharpen some of the resonances which were broadened at room temperature (those of the cis conformers). The structural assignments of each conformer were made by using two-dimensional NMR techniques, and the data are given in the Supporting Information. The ROESY spectrum contained predominantly intraresidue cross-peaks and some exchange peaks (only observed between the resonances of the cis conformers), indicating that the measurement of *J* couplings was required to determine structural details concerning the *ox*-[Cys-Cys] ring conformations. Because of the limited number of protons within a small organic molecule (scaffold), NOE's or ROE's provide limited information and the utilization of homonuclear and heteronuclear scalar couplings is required for structural elucidation.[17]

We were able to determine that there were two cis amide conformers by their $H_\alpha-H_\alpha$ ROE cross-peaks, and two trans amide conformers by their lack of $H_\alpha-H_\alpha$ ROE cross-peaks. The ROE from the acetyl methyl protons to the amide proton readily distinguished the *N*-terminal cysteine (Cys1) from the *C*-terminal cysteine (Cys2). In summary, the ROESY and TOCSY experiments indicated there were four observed conformations for compound **2**: two having trans amide bonds (designated T$-$ and T$'-$) with a ratio of 47:15, and two conformers containing cis amide bonds (designated C$+$ and C$-$) with a ratio of 29:9.[18]

The H$-$C heteronuclear one-bond correlated spectrum showed complete resolution of the signals for the four conformers, with the exception of the acetyl methyl carbons of the cis isomers which were partially resolved. The β-carbon region (Figure 2, top spectrum) shows eight signals in the carbon dimension correlating to two β methylenes adopting four conformations.

(7) (a) Kao, P. N.; Karlin, A. *J. Biol. Chem.* **1986**, *261*, 8085−8088. (b) Avizonas, D. Z.; Farr-Jones, S.; Kosen, P. A.; Basus, V. J. *J. Am. Chem. Soc.* **1996**, *118*, 13031−13039.

(8) (a) Balass, M.; Katchalski-Katzir, E.; Fuchs, S. *Proc. Natl. Acad. Sci.* **1997**, *94*, 6054−6058. (b) Kasher, R.; Balass, M.; Scherf, T.; Fridkin, M.; Fuchs, S.; Katchalski-Katzir, E. *Chem. Biol.* **2001**, *8*, 147−155. (c) Bracci, L.; Lozzi, L.; Lelli, B.; Pini, A.; Neri, P. *Biochemistry* **2001**, *40*, 6611−6619.

(9) Walker, J. W.; Lukas, R. J.; McNamee, M. G. *Biochemistry* **1981**, *20*, 2191−2193.

(10) Mishina, M.; Tobimatsu, T.; Imoto, K.; Tanaka, K.-I.; Fujita, Y.; Fukuda, K.; Kurasaki, M.; Takahashi, H.; Morimoto, Y.; Hirose, T.; Inayama, S.; Takahashi, T.; Kuno, M.; Numa, S. *Nature* **1985**, *313*, 364−369.

(11) Schiering, N.; Kabsch, W.; Moore, M. J.; Destefano, M. D.; Walsh, C. T.; Pai, E. F. *Nature* **1991**, *352*, 168−172.

(12) Bodanszky, M.; Stahl, G. L. *Proc. Natl. Acad. Sci., U.S.A.* **1974**, *71*, 2791−2794.

(13) Smit, A. B.; Syed, N. I.; Schaap, D.; Minnen, J. v.; Klumperman, J.; Kits, K. S.; Lodder, H.; Schors, R. C. v. d.; Elk, R. v.; Sorgedrager, B.; Brejc, K.; Sixma, T. K.; Geraerts, W. P. M. *Nature* **2001**, *2001*, 261−268.

(14) Brejc, K.; Dijk, W. J. v.; Klaassen, R. V.; Schuurmans, M.; Osst, J. v. d.; Smit, A. B.; Sixma, T. K. *Nature* **2001**, *411*, 269−276.

(15) (a) Capasso, S.; Mazzarella, L.; Tancredi, T. *Biopolymers* **1979**, *18*, 1555−1558. (b) Capasso, S.; Mazzarella, L.; Tancredi, T.; Zagari, A. *Biopolymers* **1984**, *23*, 1085−1097. (c) Garcia-Echeverria, C.; Rich, D. H. *Pept. Chem., Struct. Biol., Proc. Am. Pept. Symp. 13th* **1994**, *13*, 782−784. (d) Sukumaran, D. K.; Prorok, M.; Lawrence, D. S. *J. Am. Chem. Soc.* **1991**, *113*, 706−707.

(16) (a) Karplus, M. *J. Chem. Phys.* **1959**, *30*, 11−13. (b) Karplus, M. *J. Am. Chem. Soc.* **1963**, *85*, 2870−2871. (c) The general form of the Karplus equation is the following: $^3J = A' \cos^2\theta - B' \cos\theta + C'$. For a classic treatise on the use of the Karplus equation applied to peptides see: Bystrov, V. F. *Prog. NMR Spectrosc.* **1976**, *10*, 41−81.

(17) Pellegrini, M.; Weitz, I.; Chorev, M.; Mierke, D. F. *Lett. Peptide Sci.* **1998**, *5*, 151−153.

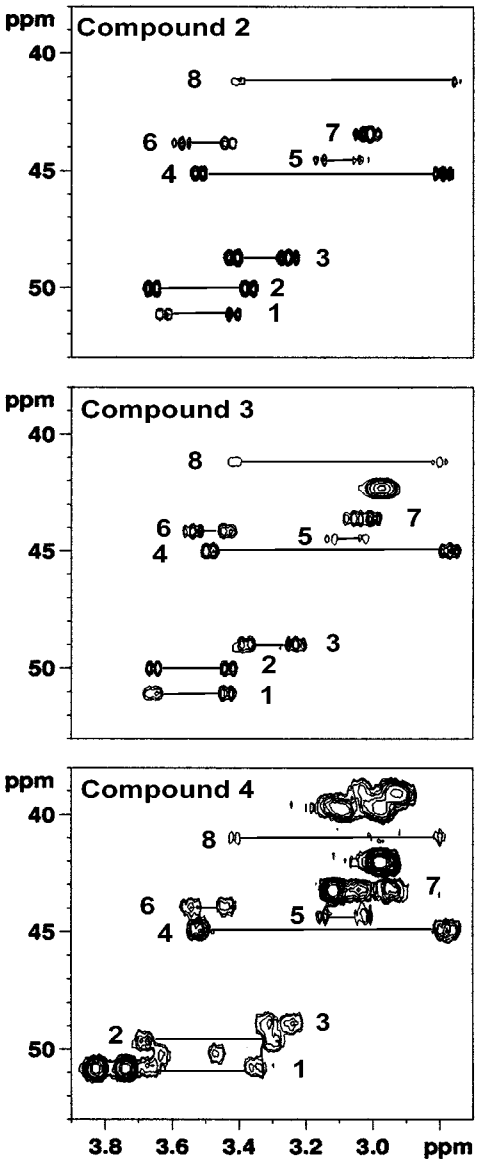

Figure 2. $^{1}H-^{13}C$ correlated NMR spectra showing (from top to bottom) the β-methylene region of Ac-*ox*-[Cys-Cys]-NH_2 (**2**), human α_7 nAChR$^{211-214}$ (**3**), and human α_7 nAChR$^{206-216}$ (**4**).

The chemical shifts for the C_β carbons of the cis conformers (signals 4, 5, 7, and 8) are all less than 46 ppm, whereas the trans conformers (signals 1, 2, and 3) are greater than 48 ppm, with the exception of the minor trans isomer's Cys2 β carbon (6). Additionally, the chemical shift separations of the trans conformer diastereotopic H_β protons are approximately 0.2−0.3 ppm, and the cis conformers each contain one pair of diastereotopic H_β protons with a large separation (0.6−0.7 ppm) and one pair of diastereotopic H_β protons with small chemical shift differences (<0.2 ppm).

We also studied the β-carbons and their attached protons for the *ox*-[Cys-Cys] of the larger peptides **3** and **4** (Figure 2, middle and bottom spectra). For **3** and **4**, resonances assigned to the non-Cys amino acids are also observed in this region, but the pattern of *ox*-[Cys-Cys] is quite distinct, and the relative conformer populations are very similar for **2**−**4**. There are only minor chemical shift differences except for the T− Cys2 H_β protons of **4**, which exhibits a much smaller proton chemical shift separation. These data suggest that the conformers identified for **2** and their relative populations are formed in these larger peptide fragments, and perhaps in native nAChRs as well.

Homonuclear ($J_{H\alpha-H\beta}$) and heteronuclear ($J_{H\beta-C'}$) *J* couplings were used for defining the two-cysteine χ_1 dihedral angle for each conformer of compound **2** as listed in Table 1. The C+ Cys1 χ_1 angle could not be determined because of degeneracy of its H_β protons (signal 7 in Figure 2, top spectrum). In general the couplings had values one would expect for one of the three staggered conformers normally assumed for amino acids.[19] There were two exceptions to this: the $H_{\beta(pro-S)}-H_\alpha$ couplings of Cys1 for conformers T′− and C−. For the case of T′−, the small $H_{\beta(pro-R)}-H_\alpha$ coupling along with the large $H_{\beta(pro-R)}-C'$ coupling indicated that 60° is the value of χ_1 and the observed $H_{\beta(pro-S)}-H_\alpha$ coupling constant (5.5 Hz) is anomalously large. For the C− conformer, since $H_{\beta(pro-R)}-H_\alpha$ had the maximum coupling value, the 5.2 Hz $H_{\beta(pro-S)}-H_\alpha$ coupling was unusually high. The needed heteronuclear coupling could not be measured so that C− Cys1 χ_1 was assigned a value of either 180° or −60°.

For defining the ϕ_2 dihedral angle for each conformer homonuclear ($J_{HN2-H\alpha2}$) and heteronuclear ($J_{HN2-C'2}$, $J_{H\alpha2-C'1}$ and $J_{HN2-C\beta2}$) coupling constants were used (see Table 2). The homonuclear amide proton to α proton couplings for T− and C+ were uniquely positioned on the Karplus curve so that ϕ_2 could readily be assigned a value of −120°. The $J_{HN2-H\alpha2}$ coupling constants for T′− and C− gave multiple possible values for ϕ_2, therefore heteronuclear coupling constants were used.

Of the eight dihedral angles that define the *ox*-[Cys-Cys] ring, we defined four of them (ω_2, ϕ_2, and two χ_1's) by NMR. Computational methods were needed to define ψ_1, and the Cys1 and Cys2 χ_2 for the cases of $\chi_3 = +90°$ and −90°.

Computer Simulations. Low-energy conformations for *ox*-[Cys-Cys] were computed using a Monte Carlo conformational search followed by energy minimization. Multiple independent simulations were carried out in order to ensure, as far as possible, that the Monte Carlo simulations had converged to the global minimum. Since three independent Monte Carlo simulations gave the same global minimum, it is very likely that the conformational space of **2** has been thoroughly explored. The calculations provided putative low-energy structures that were manually matched with the NMR results to select the preferred solution conformations. Representative low-energy conformations for **2** are given in Table 3. These conformations can be broken into the following primary groups: T+, T−, C+, and C−.

In the case of the trans isomer, there is flexibility in the conformation of the backbone amide inside the eight-membered ring (T′+ and T′−). This amide can adopt a conformation where the carbonyl is eclipsing the first Cα hydrogen or the *N*-terminal amide. This same degree of flexibility in the endocyclic amide conformation is not observed for the cis isomer. Included in Table 3 are values determined from the *ox*-[Cys-Cys] ring from the crystal structure of the AChBP.[14] The Monte Carlo calculations produced six conformations for the cis and trans amide that are within 3.5 kcal/mol of the global minimum. In the case of the cis isomer the two lowest energy conformations have χ_1 and ϕ_2 dihedral angles that are consistent with the two observed cis conformations in the NMR. These two conformations shown in Figure 3 are the only ring conformations identified by the Monte Carlo simulation that are within 10 kcal/mol of the global minimum for the cis amide. Given the relatively small differ-

(18) The + and − refers to the positive or negative helicity associated with the disulfide bond.

(19) (a) Pachler, K. G. R. *Spectrochim. Acta* **1963**, *19*, 2085−2092. (b) Pachler, K. G. R. *Spectrochim. Acta* **1964**, *20*, 581−587. (c) Kessler, H.; Griesinger, C.; Wagner, K. *J. Am. Chem. Soc.* **1987**, *109*, 6927−6933. (d) Cung, M. T.; Marraud, M. *Biopolymers* **1982**, *21*, 953−967.

Table 1. Homonuclear and Heteronuclear Scalar Coupling Constants Used To Define χ^a of **2**

conformer	residue	^3J coupling constant (*Hz*) $H_\alpha-H_{\beta(pro-S)}$	$H_\alpha-H_{\beta(pro-R)}$	$H_{\beta(pro-S)}-C'$	$H_{\beta(pro-R)}-C'$	dihedral χ_1 (deg)
T−	Cys1	2.9	≈2.0[d]	<0.5	7.0	60
	Cys2	12.5	≈2.0	1.0	nd[e]	−60
T′−	Cys1	5.5	≈2.0	nd	7.0	60
	Cys2	12.1	3.2	2.0	nd	−60
C+	Cys1	deg[f]	deg	deg	deg	unknown
	Cys2	12.7	3.1	1.3	nd	−60
C−	Cys1	5.2[b]	12.1[c]	overlap[g,b]	nd[c]	180 or −60
	Cys2	13	≈2.0	nd	2.0	−60

[a] χ_1 was determined by the modified Karplus equation.[16c,19c] [b] Hβ is the low-field resonance. [c] Hβ is the high-field resonance. [d] ≈2.0 indicates coupling was observed and $J \cong$ line width. [e] nd indicates that the heteronuclear cross-peaks were not observed and thus the coupling was assumed to be negligible. [f] deg indicates the resonances are degenerate [g] Could not be resolved because it was too close to the T′− Cys1 C′ resonance.

Table 2. Homonuclear and Heteronuclear Scalar Coupling Constants Used To Define ϕ_2 of **2**

conformer	residue	^3J coupling constant (Hz) $H_N2-H_\alpha2$	$H_N2-C_\beta2$	$H_N2-C'2$	$H_\alpha2-C'1$	dihedral ϕ_2 (deg)
T−	Cys2	10.9	1.9	nd	1.7	−120
T′−	Cys2	6.9	nd	3.5	8	34
C+	Cys2	11.7	nd	1	2	−120
C−	Cys2	8.8	nd	2	nd	−148

Table 3. Dihedral Angles (deg) and Energies (kJ/mol) for Computed Low-Energy Conformations of **2**

isomer	energy	ϕ_2	Cys1 χ_1	Cys2 χ_1	S−S χ_3	ψ_1
T+	−428.7	−168	166	43	86	−69
T−	−427.8	−133	61	−54	−98	−40
T′+	−414.6	−6	−173	50	94	179
T′−	−414.0	70	76	−50	−85	−178
C+	−426.6	−133	−162	−50	94	155
C−	−423.2	−145	172	−83	−93	142
ox-[Cys-Cys], crystal structure, AChBP[14]	na	−127	68	−39	−97	−38

ences in the backbone and χ_1 dihedral angles along with the calculated energy differences it is difficult to unambiguously assign the major and minor cis conformer by using computer simulations. However, the NMR and molecular modeling data for the major cis conformer are most consistent with C+.

The calculated conformations involving the trans-amide have two lower energy trans conformers (T+, T−) and two higher energy conformers (T′+, T′−), but only two trans amide ring conformations are observed by NMR. Comparison of the experimental coupling constants (Tables 1 and 2) with the calculated dihedral angles (Table 3) shows that the second trans-amide conformation (T−) is consistent with the major trans conformer observed via NMR. However, the assignment of the minor trans conformer does not correspond to the other χ_3 rotamer (T+) but rather the experimental data fits T′−. Instead of the S−S dihedral angle flipping as reported previously, the observed coupling constants and computer simulations support a flip of the backbone relative to the T− conformer. The T− and T′− conformers are stable, low-energy forms and are not in fast exchange with the other calculated trans conformers since the coupling constants for determining χ_1 do not show averaged values as would be required if this type of exchange were occurring.

The calculations indicate that the backbones of the four observed conformers are relatively extended with the exception of T−, and this result is borne out experimentally by the observation of an ROE between the Cys1 H_N and the Cys2 H_N. T− is a compact structure and approximates a Type VIII β-turn.[20] Of the four dihedral angles used to define this β-turn, ψ_2 (25°) fails to meet the required value of 120°. The fact that ψ_2 falls outside the normal range for a type VIII β-turn is probably not significant since rotation of the exocyclic amide is not constrained as it would be in the native protein. The four conformations supported by the spectral data and the Monte Carlo calculations are T′−, T− (trans), and C+ and C− (cis), shown graphically in Figure 3.

In the 2-dimensional NMR proton−carbon analysis, we were able to assign every one of eight pairs of β methylenes of **2** to each of the four conformations (two per conformation). The pattern observed in the 2-D NMR for **2** was qualitatively the same for the tetrapeptide **3** and undecapeptide **4**, indicating that the conformational preferences seen for the smaller model compound were retained as additional amino acids were added. As **3** and **4** are sequences found in the α_7 nAChR, it is possible that the conformational manifold adopted for *ox*-[Cys-Cys] in that protein is similar as well.

The crystal structure of *tert*-butyloxycarbonyl-L-cysteinyl-L-cysteine disulfide methyl ester (Boc-*ox*-[Cys-Cys]-OMe) was consistent with the C+ conformer.[21] The relevant dihedral angles for comparison ($\psi_1 = 153$, $\phi_2 = -136$, Cys1 $\chi_1 = -164$, and Cys2 $\chi_1 = -59$) showed excellent agreement with the experimental observations for the C+ conformer. The Boc-*ox*-[Cys-Cys]-OMe crystals were formed by slow evaporation from a mixture of ethyl acetate and chloroform. The monomers are arranged in a head-to-tail fashion with alternating hydrophobic-hydrogen bonding interactions for stabilizing the lattice. That the crystal favors the cis amide form is assumed to be a result of conformational preference in organic solvent. In a solution of 30% methanol/70% water, the cis amide form of TCCPD[7b] slightly predominates over the trans amide form, supporting the assumption that organic solvents preferentially stabilize the cis amide in the case of *ox*-[Cys-Cys].

The crystal structure of the soluble acetylcholine-binding protein (AChBP) of the snail *Lymnaea stagnalis* has recently been determined.[14] This protein lacks the transmembrane and intracellular domains normally found for nAChRs, but is closely related to native nAChRs and binds known nAChR agonists and antagonists. A vicinal disulfide *ox*-[Cys^{187}-Cys^{188}] is found in the turn region of a loop in the cleft of the AChBP between two adjacent protein subunits, which we have determined satisfies the requirements for a type VIII β-turn structural element. When we overlay our four conformations onto this unit, the T− conformation is nearly identical (Figure 4). As the crystal structure of the AChBP does not include ACh or

(20) (a) Wilmot, C. M.; Thornton, J. M. *Protein Eng.* **1990**, *3*, 479−493. (b) Hutchinson, E. G.; Thornton, J. M. *Protein Sci.* **1994**, *3*, 2207−2216.

(21) Hata, Y.; Matsuura, Y.; Tanaka, N.; Ashida, T.; Kakudo, M. *Acta Crystallogr.* **1977**, *B33*, 3561−3564.

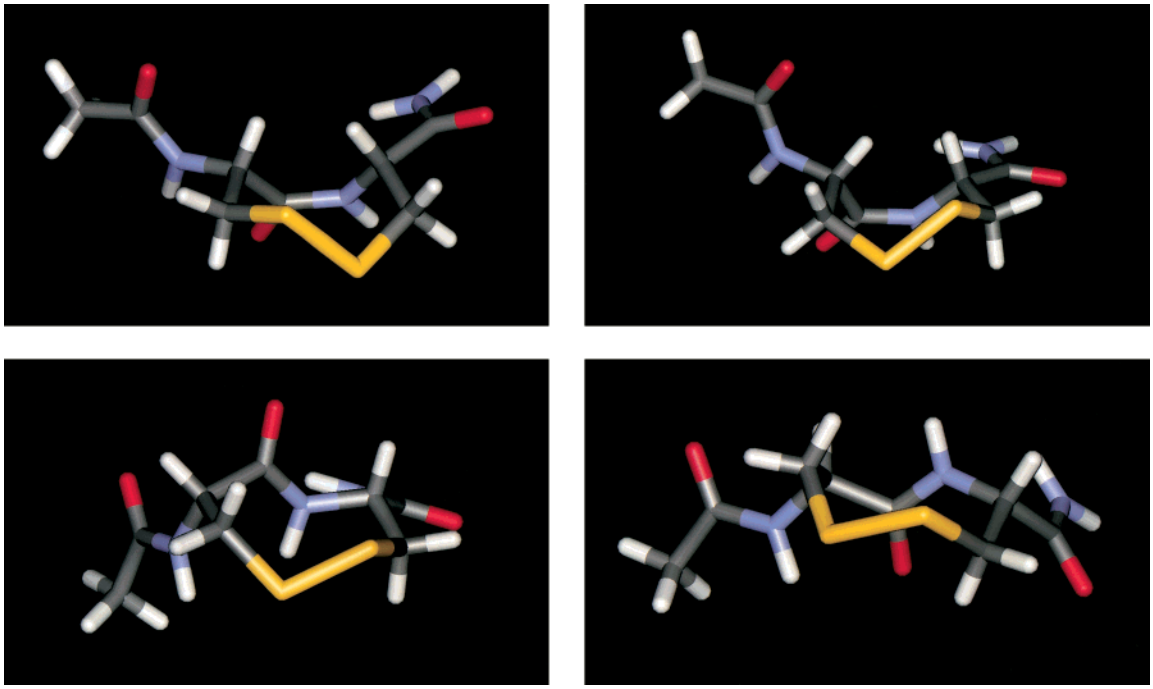

Figure 3. Conformers of Ac-*ox*-[Cys-Cys]-NH_2 (**2**): C+ (top left), C− (top right), T− (bottom left), and T′− (bottom right).

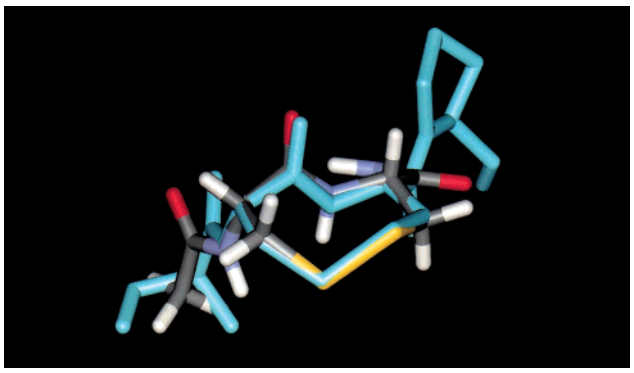

Figure 4. Overlap of *ox*-[Cys-Cys] found in the AChBP[14] (blue) and the T− conformation of compound **2** (multicolored).

another ligand, the T− conformation may represent the unliganded or uncomplexed state of *ox*-[Cys-Cys] in the AChBP protein.

What is the possible significance of conformational changes involving *ox*-[Cys-Cys] as a switch controlling nAChR function? The isomerization of the disulfide between the two observed cis isomers is expected to be relatively insignificant because the backbone for the two isomers is largely unchanged and the spatial orientation of the side chains is very similar. The most significant structural difference among the conformers is the orientation of the backbone of the ring. Based on the crystal structure, the T− conformer produces a much more compact orientation of the pendant amino acid groups. Switching between T− and the T′− or either C conformer would alter the protein conformation and topology dramatically. The cis isomers present both a hydrogen bond donor and acceptor on the same face of the backbone, whereas the trans isomers present either a hydrogen bond donor (T−) or a hydrogen bond acceptor (T′−)

Conclusion

The nAChRs are important ligand gated ion channels that mediate intracellular communication. The α7 nAChR is a high-affinity receptor for β-amyloid$_{1-42}$, and mediates calcium homeostasis and ACh release. It is important to understand the conformational preference adopted by nAChRs, to modulate their activity by the design of appropriate therapeutic agents.

The *ox*-[Cys-Cys] fragment **1** adopts four conformations in water. The lowest energy structure bears a trans amide bond with a minus helicity of the disulfide. The next lowest energy conformer was the cis amide ring with a plus helicity of the disulfide. Both of these conformers exist in a 3:1 ratio with their minor trans or cis conformer. The ratio of trans to cis amides was 1.5:1, suggesting only small energy differences between the two populations as affirmed by the computational results which showed only small differences between the various low-energy conformers. It is noteworthy that at room temperature the resonances of the cis conformers were broadened due to exchange between the plus and minus forms of the disulfide helicity. Alternatively, the trans conformers' resonances were not broadened by exchange at room temperature with the minus helicity of the disulfide being the most favored.

The unliganded conformation of *ox*-[Cys-Cys] in the closed nAChR may be similar to the type VIII β-turn found in the unliganded AChBP, which we have characterized as T− in Ac-*ox*-[Cys-Cys]-NH_2. Alternatively, the binding of ACh or other ligands could alter the conformation of *ox*-[Cys-Cys] to T′−, C+, or C− which are no longer β-turns but adopt a more extended structure.

Experimental Section

Synthetic Chemistry. Peptides were synthesized by stepwise solid-phase techniques by using an Applied Biosystems 431A peptide synthesizer with Boc/benzyl protection scheme, the *p*-methylbenzhydrylamine resin (HCl salt; Applied Biosystems), and 2-(1*H*-benzotriazol-1-yl)-1,1,3,3-tetramethyluronium hexafluorophosphate (HBTU) activation. The peptides were cleaved from the resin by treatment with HF/anisole for 1 h at −6 °C. The cleaved product was precipitated with ethyl ether and subsequently washed an additional two times in cold ethyl ether. The peptides were cyclized at a concentration of 0.5 mg/mL in a solution of 0.1 M ammonium bicarbonate. After confirmation of cyclization by HPLC and mass spectrometry, the peptide solution was acidified with trifluoroacetic acid. Each peptide was purified to homogeneity by reverse-phase high-performance liquid chromatography

(HPLC) by using two Vydac C18 columns in tandem (No. 218TP1022). A gradient of water−acetonitrile with 0.1% trifluoroacetic acid was employed to elute the peptides from the columns. Purified peptides were checked for purity by analytical HPLC on a Vydac C18 column (No. 218TP54) by using the same buffer system described for the preparative purification. Molecular weights of the purified peptides were confirmed by positive-mode ion-trap mass spectrometry (Finngan LCQ instrument).

Nuclear Magnetic Resonance Spectroscopy. The NMR sample consisted of ca. 5 mg of **2** dissolved in 500 μL of water with an additional 50 μL of D_2O for lock stabilization. The pH of the sample was 3.0. Proton and carbon spectra were referenced to TSP. Data were collected on a Bruker DMX 600 MHz NMR spectrometer with a triple resonance (H, C, N) and triple axis gradient probe maintained slightly above the freezing point (∼0 °C). The gradient amplifier was an Accustar 3 delivering 10 amps per channel. For the proton experiments, water suppression was accomplished by using presaturation or Watergate[22] with magic angle gradients (∼10 G/cm, 1 ms rectangular pulses) in combination with either the 3−9−19[23] or the selective 90−180−selective 90[22] degree pulse combinations. TOCSY[24] spectra were collected by using a Z-filtered DIPSI2 sequence[25] along with weak gradient purge pulses (∼3 G/cm, 1 ms sine shaped pulses) during the z-filter delays. A time of 60 ms was used for the isotropic mixing period. The ROESY[26] sequence used was the frequency offset compensated version of Griesinger and Ernst[27] in which the CW spin-locking field (∼3.1 kHz) is bracketed by hard 90° pulses, and a mixing time of 250 ms was used. The proton spectra were collected by using 32 to 96 scans per increment and 256 complex points in t_1 and 2048 complex points in t_2 (11 ppm sweep width). Quadrature detection in the indirect dimension was accomplished by using TPPI or States-TPPI methods. Spectra were zero-filled twice in the indirect dimension and apodized with 90° shifted sine squared functions in both dimensions. Baselines were flattened in one or both dimensions.

One-bond proton−carbon correlations were obtained by using a sensitivity enhanced HSQC type sequence[28] without additional water suppression. Sine shaped, magic angle gradients of 750 ms duration were used in a 4:1 (57:14.25 G/cm) ratio for the coherence selection. The proton sweep width was 6 ppm and the carbon sweep width was 50 ppm for the dipeptide and tetrapeptide and 130 ppm for the undecapeptide. There were 128 increments (64 or 128 scans per increment) in the indirect dimension and 2048 points in the direct dimension. Data were zero filled once in F2 and the points doubled in F1 by using linear prediction and zero filled once. Echo−antiecho processing[29] was used to generate quadrature in F1 and both dimensions were multiplied by 90° shifted sine squared functions. Long-range proton−carbon correlations were recorded by using a gradient version of the HMBC experiment[30] with a weak CW field (13 Hz) to further reduce the water resonance during the recycle delay. A delay of 65 ms was used for the evolution of the long-range heteronuclear coupling. Similar experimental parameters were used as in the one-bond heteronuclear correlated experiments except the carbon dimension was 170 ppm and a full proton sweep width was used (11 ppm). The data were processed in the magnitude mode by using a 0° sinebell in both dimensions. Heteronuclear coupling constants were measured by using a phase sensitive HMBC[31] and the HSQMBC experiment of Williamson.[32] These experiments were acquired by using higher resolution in both dimensions (ps-HMBC: 10 ppm proton sweep width with 4096 complex data points and a 175 ppm carbon sweep width with 256 scans per each of 320 increments; HSQMBC: 9 ppm proton sweep width with 4096 complex data points and a twice folded 50 ppm carbon sweep width with 256 scans per each of 256 increments). The gradient ratios used were those prescribed in the original papers except that we used magic angle gradients. The spin lock purge used in the HSQMBC was 2.05 ms. Minor changes to both sequences include the incorporation of composite carbon 180° pulses ($90_x-180_y-90_x$)[33] and deletion of the TANGO pulse sandwich in the HSQMBC (refer to Figure 1C of Williamson et al.[32]). Both experiments used the echo−antiecho data collection scheme to generate quadrature in F1. Both dimensions were apodized with 90° sine squared functions. The processed spectra were linear predicted and zero filled to 16K by 2K data points by using strip transforms to facilitate data handling. The heteronuclear couplings were measured following published peak fitting methods.[34]

Molecular Modeling. Simulations for **2** were carried out by using the OPLS all atom force field,[35] as implemented in MacroModel.[36] Since the objective was to model the aqueous conformations, we also included solvation using the GB/SA water model.[37] GB/SA has been found to give excellent average solvation free energies when used in combination with OPLS.[38] The Monte Carlo search algorithm implemented in MacroModel was used to search the conformational space for both the cis and trans endocyclic amide. In each case (cis and trans), the structure was subjected to three independent Monte Carlo simulations. Each Monte Carlo simulation was run for 5000 search steps. At each step in the Monte Carlo simulation the resulting conformations were subjected to minimization for a maximum of 750 cycles. All unique structures that satisfied an energy cutoff of 12 kcal/mol relative to the global minimum (lowest energy conformation) were saved for analysis. The use of multiple independent simulations provides a means for ensuring that the Monte Carlo calculations have converged. If they all result in the same global minimum we can have a high degree of confidence that the conformational space has been adequately explored. The calculated low-energy structures were manually matched with the NMR results to select the preferred solution conformations. The homonuclear proton−proton $^3J_{\alpha-\beta}$ couplings were used to quickly filter the calculated structures and then a more thorough comparison was done to find the calculated conformers that were consistent with all of our experimental observations.

Acknowledgment. We thank Dr. R. Thomas Williamson (Wyeth-Ayerst Research) for a version of his HSQMBC sequence along with some processing suggestions. We also acknowledge technical support by Anita Emerson and Perry Leung of our peptide synthesis laboratories (R. W. Johnson PRI, La Jolla).

Supporting Information Available: Additional NMR data and computer simulations (MOL files for the four conformers: C+, C−, T− and T′−) (PDF). This material is available free of charge via the Internet at http://pubs.acs.org.

JA016505M

(22) Piotto, M.; Saudek, V.; Sklenar, V. *J. Biomol. NMR* **1992**, *2*, 661−665.
(23) Sklenar, V.; Piotto, M.; Leppik, R.; Saudek, V. *J. Magn. Reson., Ser. A* **1993**, *102*, 241−245.
(24) Braunschweiler, L.; Ernst, R. R. *J. Magn. Reson.* **1983**, *53*, 521−528.
(25) Rance, M. *J. Magn. Reson.* **1987**, *74*, 557−564.
(26) Bax, A.; Davis, D. G. *J. Magn. Reson.* **1985**, *63*, 207−213.
(27) Griesinger, C.; Ernst, R. R. *J. Magn. Reson.* **1987**, *75*, 261−271.
(28) Schleucher, J.; Schwendinger, M.; Sattler, M.; Schmidt, P.; Schedletzky, O.; Glaser, S. J.; Sorensen, O. W.; Griesinger, C. *J. Biomol. NMR* **1994**, *4*, 301−306.
(29) Palmer, A. G., III; Cavanagh, J.; Wright, P. E.; Rance, M. *J. Magn. Reson.* **1991**, *93*, 151−170.
(30) Summers, M. F.; Bax, A. *J. Am. Chem. Soc.* **1986**, *108*, 2093−2094.
(31) Cicero, D. O.; Barbato, G.; Bazzo, R. *J. Magn. Reson.* **2001**, *148*, 209−213.
(32) Williamson, R. T.; Marquez, B. L.; Gerwick, W. H.; Kover, K. E. *Magn. Reson. Chem.* **2000**, *38*, 265−273.
(33) Levitt, M. H.; Freeman, R. *J. Magn. Reson.* **1979**, *33*, 473−476.
(34) (a) Sheng, S.; Halbeek, H. *J. Magn. Reson.* **1998**, 130, 296−299. (b) Titman, J. J.; Neuhaus, D.; Keeler, J. *J. Magn. Reson.* **1989**, *85*, 111−131.
(35) (a) Jorgensen, W. L.; Tirado-Rives, J. *J. Am. Chem. Soc.* **1988**, *110*, 1657−1666. (b) Jorgensen, W. L.; Maxwell, D. S.; Tirado-Rives, J. *J. Am. Chem. Soc.* **1996**, *118*, 11225−11236.
(36) (a) MacroModel, Schrodinger Inc., Version 7.0, 1999. (b) Mohamadi, F.; Richards, N. G. J.; Guida, W. C.; Liskamp, R.; Lipton, M.; Caufield, C.; Chang, G.; Hendrickson, T.; Still, W. C. *J. Comput. Chem.* **1990**, *11*, 440.
(37) (a) Qiu, D.; Shenkin, P. S.; Hollinger, F. P.; Still, W. C. *J. Phys. Chem. A* **1997**, *101*, 3005−3014. (b) Still, W. C.; Tempczyk, A.; Hawley, R.; Hendrickson, T. *J. Am. Chem. Soc.* **1990**, *112*, 6127−6129.
(38) Reddy, M. R.; Erion, M. D.; Agarwal, A.; Viswanadhan, V. N.; Mcdonald, D. Q.; Still, W. C. *J. Comput. Chem.* **1998**, *19*, 769−780.